

PAPER



Cite this: *Green Chem.*, 2020, **22**, 1366

CO₂ and CH₄ conversion in “real” gas mixtures in a gliding arc plasmatron: how do N₂ and O₂ affect the performance?†

Joachim Slaets, * Maryam Aghaei,  Sara Ceulemans, Senne Van Alphen  and Annemie Bogaerts *

In this paper we study dry reforming of methane (DRM) in a gliding arc plasmatron (GAP) in the presence of N₂ and O₂. N₂ is added to create a stable plasma at equal fractions of CO₂ and CH₄, and because emissions from industrial plants typically contain N₂, while O₂ is added to enhance the process. We test different gas mixing ratios to evaluate the conversion and energy cost. We obtain conversions between 31 and 52% for CO₂ and between 55 and 99% for CH₄, with total energy costs between 3.4 and 5.0 eV per molecule, depending on the gas mixture. This is very competitive when benchmarked with the literature. In addition, we present a chemical kinetics model to obtain deeper insight in the underlying plasma chemistry. This allows determination of the major reaction pathways to convert CO₂ and CH₄, in the presence of O₂ and N₂, into CO and H₂. We show that N₂ assists in the CO₂ conversion, but part of the applied energy is also wasted in N₂ excitation. Adding O₂ enhances the CH₄ conversion, and lowers the energy cost, while the CO₂ conversion remains constant, and only slightly drops at the highest O₂ fractions studied, when CH₄ is fully oxidized into CO₂.

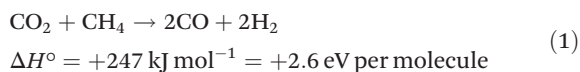
Received 31st October 2019,
Accepted 29th January 2020

DOI: 10.1039/c9gc03743h

rsc.li/greenchem

Introduction

Global warming is one of today's major environmental problems, and is attributed to enhanced greenhouse gas (GHG) concentrations in Earth's atmosphere. In this paper we study the combined conversion of CO₂ and CH₄ into CO and H₂, also called “dry reforming of methane” (DRM) [eqn (1)]:



This reaction is highly endothermic and typically carried out at high temperature, raising the energy cost, next to the risk of coking.^{1,2}

Several different technologies are being investigated for CO₂ (and CH₄) conversion, such as thermo-, photo-, electro- or bio-chemical conversion, and various combinations, mostly with catalysis.^{1,3–5} In this paper, we focus on a different approach, *i.e.*, plasma-chemical conversion. Technologies based on electrical power, such as plasma-chemical but also electrochemical conversion, are very promising, because they can store (excess)

renewable electricity in chemical form. Moreover, plasma can easily be switched on/off, making it very promising for peak shaving and grid stabilization.¹

Plasma is an ionized gas, consisting of various species, including various molecules, radicals, ions, excited species, as well as electrons, which makes it of interest for the conversion of CO₂ and CH₄ because of its high reactivity. The applied electric energy will mainly heat the light electrons, which activate the gas molecules by ionization, excitation and dissociation, leading to various ions, excited species and radicals. The latter easily react further, forming new molecules. Thus, thermodynamically challenging reactions, such as DRM, can proceed at mild conditions of ambient pressure and temperature. Indeed, the gas does not have to be heated as a whole for the reaction to proceed, because the electrons are selectively heated, making the process more energy efficient than classical thermal conversion.¹ Therefore, DRM has been studied in a range of different plasma reactors, with promising results.¹

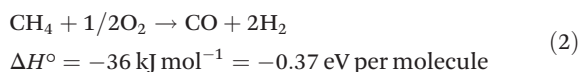
In reality, emissions from industrial plants are seldom pure, and they can contain large fractions of N₂. This is not necessarily a problem, and it was even demonstrated in various plasma types that CO₂ splitting can be enhanced upon addition of N₂.^{6–8} Moreover, N₂ can help to create a more stable plasma.

Furthermore, the DRM process in plasma was recently found to be positively influenced upon addition of O₂ to the

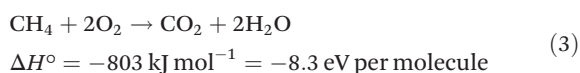
Department of Chemistry, Research Group PLASMANT, University of Antwerp, Universiteitsplein 1, 2610 Wilrijk, Belgium. E-mail: joachim.slaets@uantwerpen.be, annemie.bogaerts@uantwerpen.be

† Electronic supplementary information (ESI) available. See DOI: 10.1039/c9gc03743h

gas mixture.^{9–13} This process makes use of partial oxidation of CH₄ [eqn (2)] to enhance the conversion of CH₄ and simultaneously increase the CO and H₂ production.



Because of the negative reaction enthalpy, this reaction will occur much easier than DRM. It can make the reforming process very energy efficient and achieve a higher conversion for CH₄. However, undesired side reactions can occur. For example, complete oxidation of CH₄ [eqn (3)] should be avoided.⁹



In spite of the interesting results obtained already in literature,^{9–13} there is a clear lack in detailed understanding of the process.

In the present paper, we therefore study the conversion of CO₂ and CH₄, in the presence of both N₂ and O₂, in a gliding arc (GA) plasma reactor, more specifically a so-called gliding arc plasmatron (GAP). This reactor was developed at Drexel University by Nunnally *et al.*,¹⁴ to overcome the limitations of classical (two-dimensional) GA reactors, such as limited gas residence time in the arc.

The GAP has previously been tested for gas conversion with promising results for both CO₂ splitting and DRM.^{8,14–16} However, no stable plasma could be created for CH₄/CO₂ ratios above 1/4.

Therefore, in the present paper, we add N₂ to create a stable plasma at equal or even larger fractions of CH₄ compared to CO₂. In addition, it was recently demonstrated that N₂ could enhance the CO₂ conversion in the GAP.⁸ Furthermore, we also add O₂ in this reactor, to enhance the performance of the DRM process. We will present the conversions, product yields and energy cost of DRM, for different O₂ fractions and CH₄/CO₂ ratios.

In addition, we developed for the first time a comprehensive chemical kinetics model for this complex gas mixture, and we apply it to exactly the same conditions as in the experiments. Subsequently, we use the validated model to explain the experimental data and to provide detailed insight in the chemical composition of the plasma, and in the reaction pathways underlying the conversion process.

Experimental section

Experimental setup

The GAP reactor is schematically illustrated in Fig. 1. It exhibits a sophisticated design, based on tangential inlets, which create an initial vortex that is forced upwards along the reactor wall, which is at cathode potential (green spiral in Fig. 1). Once the end of the reactor body (cathode) is reached, the gas travels back in the other direction in a second narrower inner

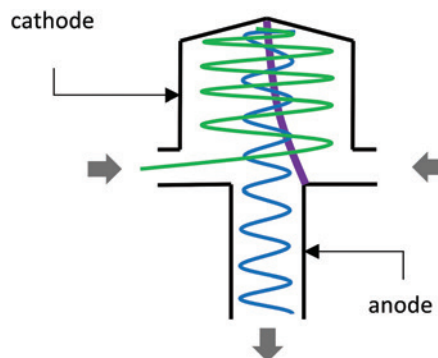


Fig. 1 Schematic picture of the GAP reactor with the outer (green) and inner (blue) vortex gas flows, the plasma arc (purple) and electrodes (black). The inlet and outlet in both reactors are indicated with arrows.

vortex (blue spiral) towards the reactor outlet, which is at anode potential, eventually leaving the reactor. A high voltage is applied between the cathode and the anode, which establishes an initial arc discharge at the shortest distance between the cathode and anode, but the arc is carried with the gas flow until it reaches the end of the cathode. Thus, the arc is positioned along the length of the reactor and stabilized in the middle of the reactor by the inner vortex flow (purple in Fig. 1). The use of an inner and outer vortex flow does not only stabilize the arc, but also allows more gas to pass through the arc and creates an isolating effect towards the reactor walls.

A schematic overview of the entire experimental setup, with gas and electrical circuit, is presented in the ESI; section 1.1, Fig. S1.† A schematic cross section of the GAP reactor, with all dimensions indicated, is also given in the ESI (Fig. S2†).

The gas composition after passing the reactor is measured with a gas chromatograph (GC) (Thermo Scientific trace 1310 GC). A detailed description of the GC measurements is given in the ESI (section 1.1†).

We tested the performance of the GAP reactor in a gas mixture of N₂, CO₂, CH₄ and O₂, studying the effect of both CH₄/CO₂ and O₂/CH₄ ratios. An overview of all conditions is given in Table S1 of the ESI.† The addition of O₂ to a mixture containing CH₄ could form an explosive mixture, which raises safety concerns. Therefore, every mixture was checked carefully to be out of the explosion regime, as explained in the ESI (section 1.2†).

For every condition, we measured the CO₂ and CH₄ conversion and the total conversion, as well as the CO and H₂ yields, with the formulas explained in the ESI (section 1.3†), based on the GC measurements with and without plasma. The experiments were performed in triplicate, and for each experiment, four GC measurements were performed, as well as six power measurements and temperature measurements. We took the weighted average of all measurements as the final result for one condition. The SEI and energy cost were determined from the power, flow rate and conversion, as explained by the formulas in the ESI (section 1.3†).

Computational part

Besides the experiments, we also developed a zero-dimensional (0D) chemical kinetics model, to obtain a better insight into the plasma chemistry occurring in the GAP reactor. This type of model has no spatial dimensions, as all plasma properties are calculated only as a function of time, hence the name zero-dimensional. However, as the arc forms a column in the middle of the reactor (see Fig. 1), which is rather uniform in the radial direction, we can describe it as a plug flow reactor (PFR), *i.e.*, we follow a volume element that flows through the arc, based on the gas flow rate. Due to the equivalence between a PFR (change in gas composition as a function of position) and a batch reactor (change as a function of time), we can translate the temporal evolution of plasma parameters, as calculated in the model, into a spatial evolution, as a function of axial position in the arc, by means of the gas flow velocity, as explained in detail in the ESI (section 2.3†). In this way, we obtain a quasi-1D model. This approach is the most suitable for the purpose of this work, as it allows to describe a detailed plasma chemistry without too much computational cost.

We used the Zero-Dimensional Plasma Kinetics solver (ZDPlasKin) to describe the plasma chemistry.¹⁷ It solves the mass conservation equations for all species taken into account in the model, based on production and loss rates, as defined by the chemical reactions. A detailed explanation is given in the ESI (section 2.1†).

The initial gas mixture consists of N₂, CO₂, CH₄ and O₂, from which many products can be formed *via* a wide range of chemical reactions. In total, we included 227 species in our model, *i.e.*, various ions, radicals, excited species and molecules, as well as the electrons. These species are listed in Table S2 of the ESI.† The chemistry in the plasma is incorporated by 16 210 reaction, *i.e.*, various electron impact reactions, electron-ion recombination reactions, ion-ion, ion-neutral, and neutral-neutral reactions, as well as vibrational-translational (VT) and vibrational-vibrational (VV) relaxation reactions. The latter are important, because we pay special attention to the vibrational levels of the various molecules, which can be important for energy-efficient CO₂ conversion, as will be explained in the Results and discussion section.

More details on the chemistry, the assumptions made in the model, the input data (such as temperature profile), and the calculation of conversion and yields in the model, both for the gas passing through the arc and outside the arc, can be found in the ESI (section 2†).

Results and discussion

We first present the measured conversions, product yields and energy cost for different gas mixing ratios, and we compare them with the corresponding calculation results. The experiments were always performed in triplicate, but the plasma was very stable, yielding only small error bars, barely visible in the figures. In addition, we also plot the calculated product yields

for those products that could not be detected experimentally, *e.g.*, because of their low concentrations. Subsequently, we will provide more detailed modelling results, including analysis of the reaction pathways, for a better understanding of the underlying chemistry.

CO₂ and CH₄ conversion

We tested two different CH₄ fractions, *i.e.*, 10 and 15%, at a constant CO₂ fraction of 10%, and we varied the O₂ fraction as much as possible, but taking care to safely stay out of the explosion regime (see details in the ESI: section 1.2†). We present the results as a function of both the O₂ fraction and O₂/CH₄ ratio, to allow for easy comparison between the experiments at different CH₄ fractions. The remaining gas fraction is N₂ (between 58.5 and 80%; see Table S1 in the ESI†). The total gas flow rate is kept fixed at 10 L min⁻¹, and the power is between 349 and 472 W (see measurements in ESI: Fig. S5†).

The measured and calculated CO₂ and CH₄ conversions are plotted in Fig. 2. The CO₂ conversion reaches values between 44 and 52%, nearly independent of the O₂ fraction, except for the 1.1 O₂/CH₄ ratio, which yields a lower CO₂ conversion of 33 and 31%, for a CH₄ fraction of 10 and 15%, respectively.

Without O₂ addition, the CH₄ conversion is 62% for 10% CH₄ in the mixture, and it slightly drops to 55%, at 15% CH₄ in the mixture. Upon O₂ addition, the CH₄ conversion rises dramatically. A maximum conversion of 98 and 99% is

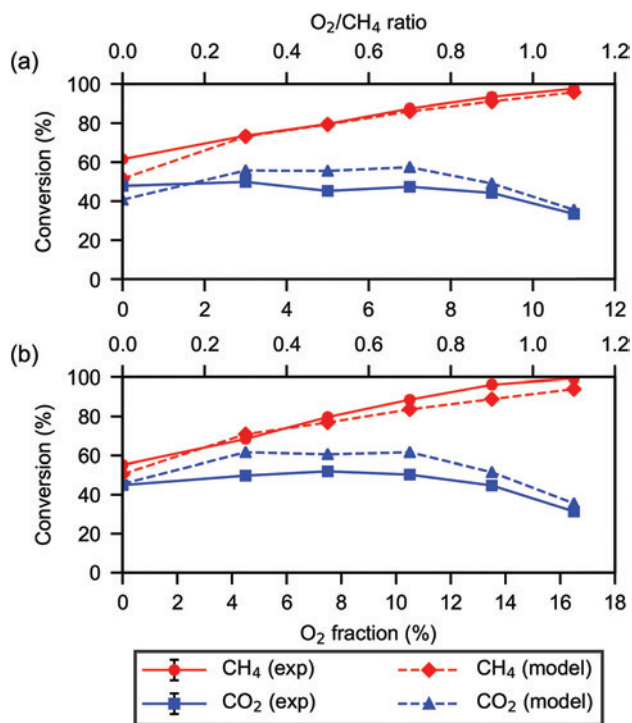


Fig. 2 Experimental and modelling results for the CO₂ and CH₄ conversion, as a function of the O₂ fraction and O₂/CH₄ ratio, for a CH₄ fraction of 10% (a) and 15% (b). The experiments were performed in triplicate, but the error bars on the experimental results are too small to be visible.

reached for 10 and 15% CH₄ fraction, respectively, at the highest O₂/CH₄ ratio of 1.1.

This high CH₄ conversion and decreasing CO₂ conversion upon rising O₂ fraction is attributed to the full oxidation of CH₄ due to O₂, producing CO₂, and thus effectively lowering the conversion of the latter. The conversions of CH₄ are significantly higher than those of CO₂, which can be explained by the higher bond strength of the C=O bond in CO₂ (*i.e.*, 5.52 eV vs. 4.48 eV for the C–H bond in CH₄),¹³ making it more difficult to be converted.

Product yields

The measured and calculated yields for CO and H₂ are depicted in Fig. 3; detailed information about the calculations is given in sections 1.3 and 2.4 of the ESI.† The CO yield ranges from 8.3 to 13% for a CH₄ fraction of 10%, and from 8.2 to 18% for a CH₄ fraction of 15%. A higher O₂ fraction enhances the formation of CO, by partial oxidation of CH₄, but for the highest O₂ fractions the yield is reduced again as a result of full oxidation. A higher CH₄ fraction enhances the CO yield for higher O₂ fractions, while it slightly reduces the CO yield when there is no O₂ present. The measured H₂ yield

ranges from 6.5 to 9.8% for 10% CH₄ and from 10 to 14% for 15% CH₄. The O₂ fraction only has a small influence on the H₂ yield, which decreases slightly towards higher O₂ fractions, while a higher CH₄ fraction results in a higher H₂ yield. Besides syngas, a major product detected in our GC is C₂H₂, which reaches its highest yield when no O₂ is present. Its yield decreases from 2.5 to 0.41% and from 4.6 to 0.40% upon increasing O₂ fraction, for a mixture with 10 and 15% CH₄, respectively.

The calculated yields are very close to the experimental values for CO and C₂H₂, but there is a significant deviation for the H₂ yield. Note that the simulations were validated by comparing the CO₂ and CH₄ conversion, but not the product yields. This is an aspect of the model that we should improve in our future research.

It is clear from our model that besides H₂ and CO, H₂O is a major product, but it could not be measured with our GC. Therefore, only the modelling results are displayed in Fig. 3, showing a yield ranging from 2.7 to 16% for 10% CH₄ and from 3.0 to 23% for 15% CH₄, *i.e.*, comparable to the CO yield. The strong increase with rising O₂ fraction is due to the full oxidation of CH₄ to CO₂, in which H₂O is produced.

Fig. 4 illustrates the calculated yields of the other products that were formed in too small quantities to be detected by our

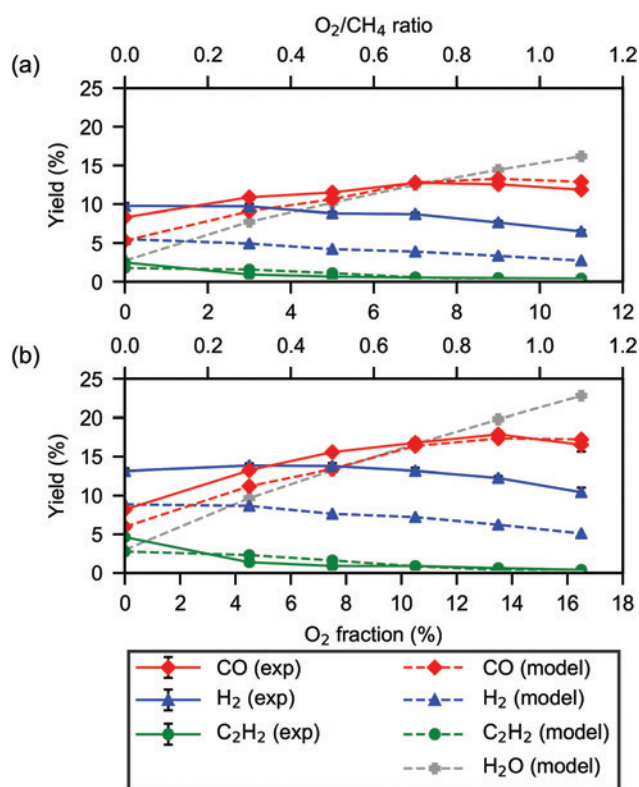


Fig. 3 Experimental and modelling results for the CO, H₂ and C₂H₂ yields and modelling results for the H₂O yield, as a function of the O₂ fraction and O₂/CH₄ ratio, for a CH₄ fraction of 10% (a) and 15% (b). The yields for CO and C₂H₂ were calculated based on carbon, while the yields of H₂ and H₂O were based on hydrogen. The experiments were performed in triplicate, but the error bars on the experimental results are too small to be visible.

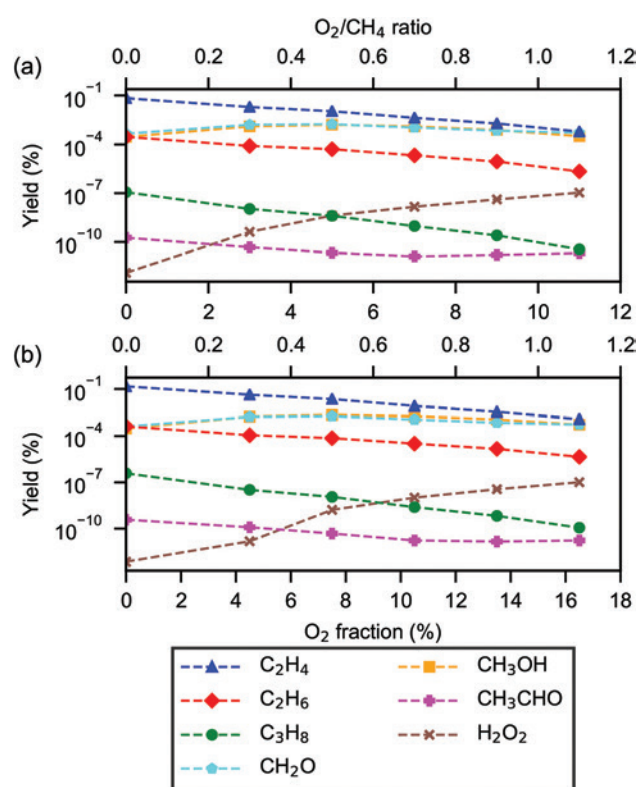


Fig. 4 Modelling results for the C₂H₄, C₂H₆, C₃H₈, CH₂O, CH₃OH, CH₃CHO and H₂O₂ yields as a function of the O₂ fraction and O₂/CH₄ ratio, for a CH₄ fraction of 10% (a) and 15% (b). The yields for all products plotted in this figure were calculated based on carbon, except for H₂O₂ which was based on hydrogen. The experiments were performed in triplicate, but the error bars on the experimental results are too small to be visible.

GC. This qualitatively correlates with our modelling results, which indeed predict that they are formed only in minor amounts. It also demonstrates the added value of modelling, to provide extra information that cannot be obtained from the experiments. The C_2H_4 , C_2H_6 and C_3H_8 yields, which are the result of CH_4 conversion, reach their maximum when no O_2 is added to the mixture. Indeed, upon O_2 addition, CH_4 is partially converted into oxygenates (including CO and CO_2), and there is less CH_4 left to be converted into hydrocarbons, and thus, the yields of these hydrocarbons decrease upon O_2 addition. The fact that C_2H_2 and C_2H_4 are the major hydrocarbons formed is in agreement with previous studies for DRM in the GAP,¹⁵ and it is beneficial, especially for C_2H_4 , which is a more valuable product for the chemical industry than *e.g.*, C_2H_6 .¹⁸

The yields of the oxygenates plotted in Fig. 4, *i.e.*, CH_2O , CH_3OH and CH_3CHO , follow different trends upon addition of O_2 . The CH_2O and CH_3OH yields show a maximum at an O_2/CH_4 ratio of 0.5. This can be explained because both O_2 and CH_4 are needed to form these oxygenates, but at too high O_2 fractions, CH_4 is further oxidized into CO_2 , as demonstrated in Fig. 2 above. Finally, the H_2O_2 yield increases continuously upon increasing O_2 fraction, as expected.

It is clear from Fig. 3 and 4 that DRM in our GAP reactor mainly produces syngas. In our future work, we want to add catalysts after the plasma reactor, to verify whether we can selectively form other compounds in higher amounts, such as light olefins or oxygenates. Note that we added O_2 to enhance the CH_4 conversion, but the O_2 was fully converted into CO (and small fractions of CO_2 , for the highest O_2 fractions), and thus no O_2 was left after the reaction. This was found both experimentally, because only trace amounts of O_2 were detected, as well as in our model. This is important, because eliminating O_2 from a syngas mixture is not straightforward, and it would make the downstream processes more expensive.

Syngas ratio

In Fig. 5, we present the measured and calculated syngas ratio, as this is an important parameter for the production of value-added chemicals, such as fuels or methanol. Our measured H_2/CO ratio varies from 1.19 to 0.56 upon increasing O_2 fraction, for the gas mixture with 10% CH_4 , and from 1.72 to 0.63 for the gas mixture with 15% CH_4 , while our calculated values are somewhat lower. This is attributed to the H_2 production that is slightly underestimated in our model. The addition of O_2 significantly reduces the H_2/CO ratio, due to the formation of more H_2O and oxygenates, as seen in Fig. 3–4 above.

Thus, our obtained syngas ratio is quite lower than the ideal syngas ratio for practical Fischer-Tropsch synthesis, which is typically between 1.7 and 2.15, depending on the catalyst and operating conditions.¹⁹ When using it for methanol synthesis, the syngas ratio needs to be even higher, *i.e.*, up to 3, which could not be reached in our experiments. However, some special catalysts can produce alcohols from a lower syngas ratio of 1.¹⁹ We believe a more suitable syngas ratio

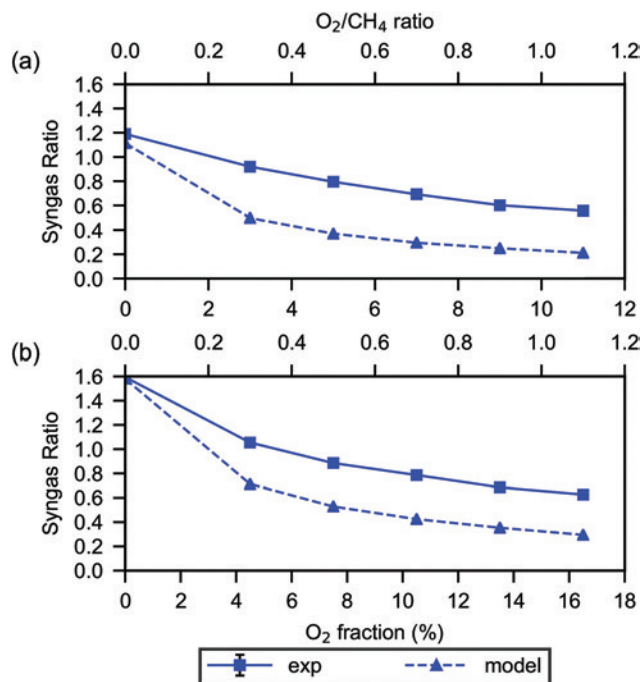


Fig. 5 Experimental and modelling results for the syngas ratio (H_2/CO), as a function of the O_2 fraction and O_2/CH_4 ratio, for a CH_4 fraction of 10% (a) and 15% (b). The experiments were performed in triplicate, but the error bars on the experimental results are too small to be visible.

could be reached when increasing the CH_4 fraction in the mixture. This is planned for our future work.

Energy cost of the conversion

The energy cost is obtained from the total conversion and the specific energy input (SEI); see formulas in the ESI (section 1.3†). The total conversion is calculated as the sum of the individual conversions of CO_2 and CH_4 , each multiplied with their fraction in the mixture, and is plotted in ESI Fig. S4†. The SEI is defined by the ratio of plasma power over gas flow rate. Both the plasma power and SEI are also plotted in the ESI (Fig. S5 and S6†), as a function of O_2 fraction and O_2/CH_4 ratio. The power ranges between 349 and 472 W for the different conditions (see measurements in ESI: Fig. S5†). Because we use a constant gas flow rate of 10 L min^{-1} in these experiments, the SEI varies around $2.1\text{--}2.8\text{ kJ L}^{-1}$ (or $0.5\text{--}0.7\text{ eV per molecule}$). The resulting energy cost is plotted in Fig. 6 for the various conditions investigated. We plot the results both in eV per molecule (left y-axis) and in kJ L^{-1} (right y-axis), because the first one is most relevant to benchmark our results with other plasma processes, while the latter one is more relevant for process chemistry.

An energy cost of 19.7 kJ L^{-1} (or 5 eV per molecule) is reached for mixtures without O_2 and a fraction of 10% CH_4 . A higher CH_4 fraction of 15% slightly increases the energy cost to 21 kJ L^{-1} (or $5.34\text{ eV per molecule}$), which is logical, because of the higher power needed to establish the plasma (see ESI Fig. S5†). When adding O_2 to the gas mixture, the

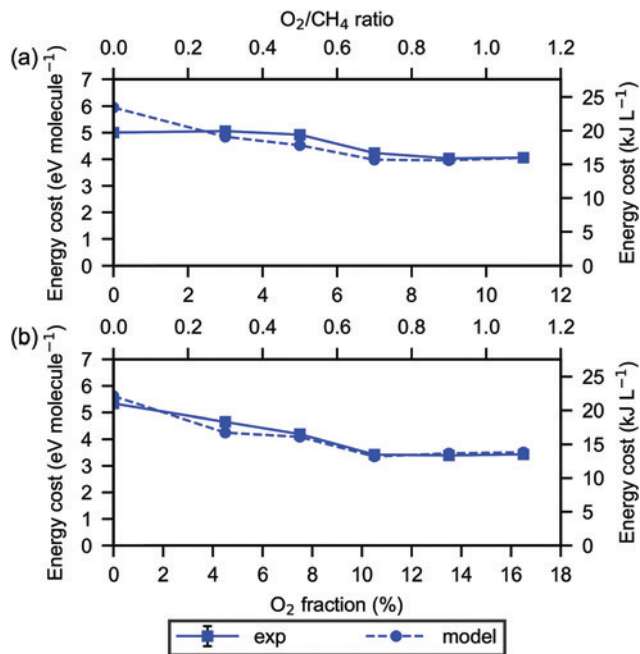


Fig. 6 Experimental and modelling results for the energy cost of the total CO₂ and CH₄ conversion, as a function of the O₂ fraction and O₂/CH₄ ratio, for a CH₄ fraction of 10% (a) and 15% (b). The experiments were performed in triplicate, but the error bars on the experimental results are too small to be visible.

energy cost decreases, reaching a minimum of 15.9 and 13.4 kJ L⁻¹ (corresponding to 4.03 and 3.39 eV per molecule) for 10 and 15% CH₄ in the mixture, respectively, at an O₂/CH₄ ratio of 0.9. The higher O₂/CH₄ ratio of 1.1 shows a somewhat higher energy cost of 16.0 and 13.5 kJ L⁻¹ (or 4.06 and 3.43 eV per molecule), for the two CH₄ fractions, due to the slightly lower total conversion (see ESI Fig. S4†).

Our results indicate that the gas mixture with 15% CH₄, and either 10.5 or 13.5% O₂ (corresponding to an O₂/CH₄ ratio of 0.7 or 0.9) yields the lowest energy cost, in combination with a high conversion of CH₄, without losing CO₂ conversion. An O₂ fraction of 16.5% also yields a low energy cost and even a slightly higher CH₄ conversion (near 100%). However, the CO₂ conversion is lower in this case, due to the full oxidation of CH₄, producing CO₂, as explained above. Higher O₂ fractions were not possible, because of risks to enter the explosion regime, and they would not give a further enhancement in CH₄ conversion, which is already near 100%, while they would further reduce the CO₂ conversion. Higher CH₄ fractions were not possible either, again because of risks to enter the explosion regime, as well as due to coking issues. These values of conversion and energy cost will be benchmarked below with literature data.

Note that our definition of energy cost does not account for heat recovery, and for the energy needed to run the reactor. Indeed, we use the plasma power as input, to allow benchmarking with other plasma processes, where this is standard practice, in order to identify the efficiency of the plasma

process itself. However, to define the real energy cost, we would need to consider the power from the wall socket. For our GAP reactor, we measured the ratio between plasma power and applied power, and obtained roughly an efficiency of 75–80%, so it means that the actual energy cost, when accounting for the efficiency of the power supply, would be a factor 1.3 higher. In addition, we don't take into account the cost of product separation, which would also add to the overall cost of the process. On the other hand, if we would be able to include heat recovery, this could reduce the overall energy cost, because our GAP reactor operates at a temperature around 1500–3000 K. We would like to investigate this in our future work.

Temperature of the gas leaving the reactor

We recorded the temperature of the gas leaving the GAP reactor with a thermocouple at a distance of 26 cm from the GAP outlet (see details in the ESI, section 1.1†). This temperature rapidly increases after igniting the plasma but stabilizes after some time. Therefore, we started the filling of the sample loops in the GC only after 10 min, to let the temperature and plasma stabilize. The observed temperature at the start and the end of the filling of the sample loops in the GC is displayed in Fig. 7. It is clear that the temperature still rises during the filling of the sample loops, meaning that the plasma was not yet fully stabilized, but this was not reflected

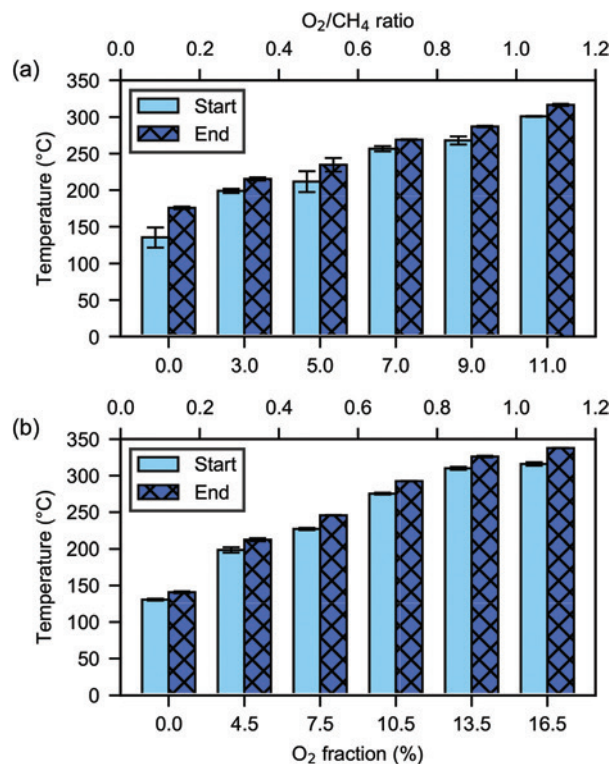


Fig. 7 Temperature of the exhaust gas flow, as a function of the O₂ fraction and O₂/CH₄ ratio, at the start and the end of the filling process of the GC sample loops, for a CH₄ fraction of 10% (a) and 15% (b).

in the GC measurements (*cf.* the very small error bars in our obtained conversions, yields and energy costs; see Fig. 2–4, 6, and ESI†). In addition, the temperature rises with increasing O₂ fraction, which is like expected, as the partial and full oxidation of CH₄ are both exothermic reactions. Without O₂, the temperature is around 150 °C, and it rises to above 300 °C for O₂/CH₄ ratio of 1.1. Increasing the CH₄ fraction from 10 to 15% shows only a minor influence on the temperature.

It should be noted that these values do not represent the plasma temperature, which is in the order of 2000–3000 K (ref. 20) (see also ESI Fig. S3†), and thus, also the temperature directly flowing out of the GAP will be higher, but it could not be measured in the experimental setup (see ESI Fig. S1†). However, the temperature values in Fig. 7 give an indication of the influence of the gas mixture on the temperature in the reactor as well. In addition, in future research, we would like to combine the GAP with post-plasma catalysis, so it will be interesting to measure the temperature as closely as possible to the GAP outlet, and at varying positions from the outlet, to determine the optimal position of a catalyst bed. Indeed, the temperature values presented in Fig. 7 indicate that heat recovery of the plasma for catalyst activation could be a viable option.

Benchmarking of our results with other research

To benchmark our results with the available literature, we compare in Table 1 our CO₂ and CH₄ conversions, energy cost and H₂/CO ratios, obtained in this gas mixture (N₂, CH₄, CO₂ and O₂), to other plasma-based DRM results in literature, *i.e.*, those obtained previously in the same GAP reactor for DRM, but without N₂ and O₂ addition (in which only CH₄/CO₂ ratios up to a maximum of 1/4 were possible),¹⁵ as well as with other plasma reactor types from literature.^{9,12,21,22} Our results yield the highest CH₄ conversion of all the available results.

When looking at the GAP reactor, it is clear that DRM without additional gases achieved much lower conversions for

both CH₄ and CO₂,¹⁵ *i.e.*, about half of what we could achieve in our work. On the other hand, the energy cost was lower than for our results. This is attributed to the overall gas mixture, only consisting of CO₂ and CH₄, where no energy had to be put into O₂ and N₂. Indeed, N₂ assists in the CO₂ conversion, as mentioned in the Introduction, and also explained below, but part of the applied electric power is also wasted into excitation and ionization of N₂, and can therefore not all be used for CO₂ and CH₄ conversion. This indicates that if the fraction of N₂ in our mixture could be reduced, while still maintaining a stable plasma, we expect to reach lower energy costs. This will be investigated in future work.

The results of the AC pulsed GA reactor show a similar trend, *i.e.*, for the same CH₄/CO₂/O₂ ratio, a much lower energy cost was obtained without N₂ present.⁹ For this reactor, lower conversions were obtained than in our work, but an exact comparison cannot be made, due to the different gas fractions and different flow rate used. The spark discharge plasma obtained a higher CO₂ conversion but lower CH₄ conversion, albeit at a low flow rate.¹² While achieving this high CO₂ conversion, the energy cost is almost twice as high compared to our results.

The DBD plasma shows similar CO₂ conversion but lower CH₄ conversion compared to our results, and a significantly higher energy cost (551 kJ L⁻¹) was obtained at a very low flow rate.²¹ The microwave plasma shows the highest CO₂ conversion, but a lower CH₄ conversion, and the energy cost is almost twice as high as for our results.²²

The reason why the energy cost in our study is quite low, especially compared to the DBD results, is attributed to the significant populations of the vibrational excitation levels of CO₂, as demonstrated in the ESI (Fig. S19†). Indeed, the reduced electric field (*i.e.*, ratio of electric field over gas number density: E/n) in a GA plasma (as well as in MW plasmas) is in the order of 50 Td, and this provides the right electron energy

Table 1 Overview of operating conditions (gas mixture, flow rate, power) and results for DRM (CO₂ and CH₄ conversion, energy cost, syngas ratio) for different plasma reactor types, as well as for conventional DRM

Reactor type	Gas mixture	Flow rate (L min ⁻¹)	Power (W)	CO ₂ conversion (%)	CH ₄ conversion (%)	Energy cost (kJ L ⁻¹ (eV per molecule))	H ₂ /CO ratio	Ref.
GAP	CH ₄ , CO ₂ , O ₂ , N ₂ (10%, 10%, 9%, 71%)	10	364	44	93	15.9 (4.0)	0.60	This work
GAP	CH ₄ , CO ₂ , O ₂ , N ₂ (15%, 10%, 13.5%, 61.5%)	10	421	45	96	13.4 (3.4)	0.68	This work
GAP	CH ₄ , CO ₂ (25%, 75%)	10	531	23	41	11.4 (2.9)	0.44	15
AC pulsed GA ^a	CH ₄ , CO ₂ , O ₂ , N ₂ (22%, 15%, 13%, 50%)	15	280	25	77	5.4 ^a (1.4)	—	9
AC pulsed GA ^a	CH ₄ , CO ₂ , O ₂ (44%, 29%, 27%)	15	280	27	81	2.6 ^a (0.65)	1 ^d	9
Spark discharge ^b	CH ₄ , CO ₂ , O ₂ (53%, 35%, 12%)	0.2	64	67	80	29.3 ^b (7.4)	1.5 ^d	12
DBD	CH ₄ , CO ₂ (50%, 50%)	0.02	107	44	73	551 ^c (140)	—	21
MW	CH ₄ , CO ₂ (60%, 40%)	0.2	60	69	71	25.6 (6.5)	1.5	22
Thermal DRM	CH ₄ , CO ₂ (50%, 50%)	0.1	—	75	68	—	0.87	23

^aThe energy cost for the formation of CO + H₂ was provided – we list here the value calculated in the same way as for our results. ^bThe energy cost for the formation of H₂ was provided – we list here the value calculated in the same way as for our results. ^cNo energy cost was provided – we list here the value calculated from their results in the same way as for our results. ^dDeduced from the graphical results in this paper.

for predominant vibrational excitation of CO₂ molecules, which is the most efficient CO₂ dissociation pathway,¹ while a DBD is typically characterized by a reduced electric field above 200 Td, causing more electronic excitation and ionization, which require more energy than strictly needed for dissociation, meaning a waste of energy, and thus a higher energy cost.¹

Fig. S7 in the ESI† provides an overview of energy cost *vs.* total conversion for DRM, for a wide range of different plasma types.¹ Our results are added to this figure, with red dots. They lie in the upper half of the GA results, with energy cost lower than the thermal conversion line, and even below the line of the efficiency target, defined in Snoeckx *et al.*¹ as a target for plasma to be competitive with other (existing or emerging) technologies. In other words, this is an improvement over thermal conversion, and even better than the defined efficiency target.¹ Of course, it must be realized that some O₂ is added here, which makes the overall reaction less endothermic, and it enhances the CH₄ conversion, thus lowering the energy cost.

The total conversion reached in our work is however still only about 20%, which is in the lower half of the GA results, and lower than for many other plasma reactors. Nevertheless, we believe this could be improved if we can reduce the N₂ fractions in the mixture, while still maintaining a stable plasma, because the latter limits the effective CO₂ and CH₄ conversions (because of their limited fractions in the mixture) and thus the total conversion.

It should be noted that comparison with literature data must be made with caution, because many papers in literature do not account for the gas expansion factor when calculating their conversions and energy costs, or at least there is no indication whether the gas expansion factor was employed, so most probably it was not accounted for. In the ESI (Fig. S8–S10†), we illustrate that this can affect the results, by overestimating the conversion and underestimating the energy cost. The effect is not so pronounced in our case, because we use a large excess of N₂, but it can be very dramatic when using a pure CO₂/CH₄ mixture (without O₂ or N₂ addition), as explained in the ESI.†

In general, we can conclude that the addition of O₂ (and to some extent N₂) to the gas mixture has a beneficial effect on DRM in the GAP, which shows competitive results compared to other gas mixtures and other types of plasma reactors.

Table 1 also shows the range of H₂/CO ratios obtained in the various plasma processes from literature, in comparison with our results. Our results yield a higher syngas ratio than previous results from the GAP, while the results obtained in an AC pulsed GA yielded a syngas ratio of 1, and in a spark discharge and MW plasma reactor, a syngas ratio of 1.5 was reached, which is more beneficial for the Fischer–Tropsch process. These results were however obtained for an inlet mixture with a low O₂ fraction or even without O₂ in the case of the MW reactor, thus forming less oxygenates and less H₂O, explaining the higher syngas ratio. In our reactor we also reached a ratio of up to 1.6 without O₂ present.

Finally, we compare our results with conventional DRM (see last row in Table 1, showing results for a Ni-based catalyst). It should however be noted that a wide range of catalytic materials is being used for DRM, so comparing with just one catalyst might not be fully representative. Nevertheless, we can conclude that the CO₂ conversion is much lower in our plasma reactor, but we achieve a higher CH₄ conversion. The syngas ratio is slightly higher for this catalyst compared to our results, but still lower than ideal for Fischer–Tropsch synthesis. Unfortunately, we could not directly compare the energy cost of conventional DRM with our results. However, Snoeckx and Bogaerts,¹ defined an efficiency target for the energy cost of 4.27 eV per molecule (which corresponds to 16.8 kJ L⁻¹) for pure plasma-based DRM to be economically viable. We can conclude that our reactor can reach this target value. The energy cost also decreases with increasing CH₄ fraction, and this could also help further improve the energy cost in the future.

As shown in previous sections, the measured conversions, H₂ and CO product yields, and energy costs were in good agreement with the calculated data, obtained with our model that we developed for this purpose, both in absolute values, as well as in the behaviour as a function of gas mixing ratios, for all gas mixtures investigated. It should be mentioned that we slightly adjusted the temperature profile, used as input in the calculations, as explained in detail in the ESI (section 2.3†), but we did not use any other fitting parameters. Thus, our model can provide a realistic picture of the plasma chemistry, and we can use it to obtain more insight in the underlying mechanisms. Indeed, the model can provide more information, apart from the conversions, product yields and energy cost, beyond what is possible to measure experimentally, and thus, it is extremely valuable to obtain more detailed insight in the process. In the following sections, we will discuss the contribution of the conversion inside and outside the arc region, as well as the populations of the CO₂ vibrational levels (crucial for energy-efficient CO₂ dissociation), both inside and outside the arc. In addition, we will elucidate the underlying mechanisms and reaction pathways to convert CO₂, CH₄ and O₂ into CO and H₂, along with the important intermediate products.

Calculated conversion inside and outside the arc region

The modelling results in Fig. 2–4 show similar values as the experimental data, which is quite impressive, in view of the complexity of the underlying plasma chemistry included in this model. However, we found that when our model only covers the arc region in the reactor, no good agreement could be reached with the measured conversions. Indeed, we had to perform additional simulations outside (but near) the arc, as explained in the ESI (sections 2.3 and 2.4†), to account for thermal conversion in this region. The combination of these two simulations provides a better approximation of the reality and a better agreement with the experimental results, as shown in detail in the ESI (Fig. S11 and S12†) for both CO₂ and CH₄ conversion. Indeed, our simulations indicate that for

all gas mixtures investigated, a large fraction of CO₂ and nearly all CH₄ in the arc is converted (see below). However, this results in only 13.8% of the overall conversion being achieved in the arc, because the latter is limited by the fraction of gas passing through the arc, obtained from 3D fluid dynamics simulations.²⁰ Thus, a large fraction of CO₂ and CH₄ is not passing through the arc, but is still converted by thermal reactions. In other words, the conversion outside the arc accounts for a larger part of the total conversion, as a result of the much larger fraction of gas that is not passing through the arc.^{15,20}

Fig. S13 and S14† plot the calculated density profiles of CO₂ and CH₄, as well as of the major products, CO and H₂, as a function of position in the reactor, both inside the arc and in the region around the arc. It is clear that CO₂ and CH₄ are almost immediately converted into CO and H₂ in the beginning of the arc column, illustrating that most of the reactions occur in the first micrometres of the arc and then reach a steady state, as the forward and reverse reactions become comparable.

Calculated vibrational distribution function (VDF) of CO₂

Fig. S11 and S12 in the ESI† illustrate that CH₄ and CO₂ are partially converted both inside and outside the arc. For CH₄, this is largely due to thermal reactions, with additional contributions of plasma-chemical reactions (induced by electrons) inside the arc, as will be explained below. However, for CO₂, the underlying processes are different, and can be explained by the vibrational excitation of CO₂. Indeed, as indicated in the Introduction and in the benchmarking above, a GA plasma exhibits quite low energy costs, in comparison to other plasma reactors (especially DBD plasmas), and this is attributed to higher populations of the vibrational excitation levels of CO₂. Especially the asymmetric stretch mode is important for energy-efficient CO₂ dissociation,¹ and therefore, our model includes all asymmetric mode levels up to the dissociation limit, *i.e.*, 21 levels in total (see details in the ESI, section 2.2†), besides four symmetric mode levels, as explained in Kozák *et al.*²⁴

Fig. S19 in the ESI† illustrates the calculated normalized densities of these 4 symmetric and 21 asymmetric vibrational mode levels, *i.e.*, so-called vibrational distribution function (VDF), as well as of the ground state of CO₂, at the end of the reactor, both inside the plasma arc and in the area around it, in comparison with the Boltzmann VDF.

Inside the arc we observe an increased population of the higher vibrational levels, relative to the Boltzmann distribution, which is beneficial for energy-efficient CO₂ splitting. This can be explained as follows: the lower vibrational levels are populated by electron impact vibrational excitation, which is a very efficient process in the GA, because the electrons have the right energy for this process, as discussed above. Subsequently, the higher vibrational levels of CO₂ are gradually populated upon collision with other vibrational levels, in so-called vibrational–vibrational (VV) relaxation reactions. This so-called ladder climbing process proceeds up to the highest

levels, with excitation energy around 5.5 eV, which easily dissociate into CO and O atoms, because this energy corresponds to the C=O bond dissociation energy. This vibrational pathway makes the CO₂ dissociation inside the arc quite energy-efficient and can explain the low energy costs obtained in our GAP reactor (*cf.* Fig. 6). Outside the arc, the VDF exhibits no enhancement compared to the Boltzmann distribution, as is clear from Fig. S19,† which points towards thermal CO₂ dissociation and the absence of the ladder climbing process.

Reaction pathway analysis of the conversion of CO₂, CH₄ and O₂ into CO and H₂

The main objective for the model is to analyse the underlying chemistry of the conversion of CO₂, CH₄ and O₂ into CO and H₂, to better understand the mechanisms, and thus to support the experiments to further improve the performance. We only focus on the reactions inside the arc, and not in the area around the arc, which does not contain electrons, and is simply characterized by thermal conversion. The detailed analysis, based on comparing the average reaction rates throughout the plasma arc of the different reactions involved for the species under study, is presented in the ESI (section 3.9†).

Based on this detailed reaction analysis, we can obtain insight in the important reaction pathways for the conversion of CO₂ and CH₄ in the presence of O₂ and N₂. We show this analysis again for the intermediate gas mixture of 73% N₂, 10% CO₂, 10% CH₄ and 7% O₂. The pathway scheme is given in Fig. 8. This is of course a simplified description of the entire chemistry occurring in the plasma.

As discussed in previous section, CO₂ is first vibrationally excited *via* electron impact collisions, as well as collisions with neutral species (M) or VV relaxations, to the lowest vibrational levels (CO₂(V₁)). This is followed by VV relaxations to populate the higher vibrational levels (CO₂(V_{>1})). Besides the asymmetric mode levels of CO₂(V_{1–21}), also the symmetric mode vibrational levels (CO₂(V_{a–d})) are populated in this manner. The VV relaxations can occur upon collision with any vibrationally excited species, but in the mixture under study, the vibrational levels of N₂ and CO are the most involved in this process for the asymmetric mode vibrational levels, while the symmetric mode levels are mostly populated by VV reactions with other CO₂ molecules. Indeed, the major role of N₂ in the mixture, besides stabilizing the plasma, as explained above, so that larger CH₄ fractions can be considered in the mixture,¹⁵ is to assist in this process of vibrational ladder climbing. Note that its dissociation into N atoms, from which other N-compounds (*e.g.*, NO_x, NH, NHO, ...) can be formed, is found to be of minor importance at the conditions under study. Therefore, only N₂, N₂(V₁) and N₂(V_{>1}), but no other N-compounds are shown in the diagram of Fig. 8. For both CO₂ and N₂, the higher vibrational levels can also relax back to lower levels, by either VV or VT (vibrational–translational) relaxations. The latter process is generally more important at higher gas temperature, and should be avoided, as it reduces

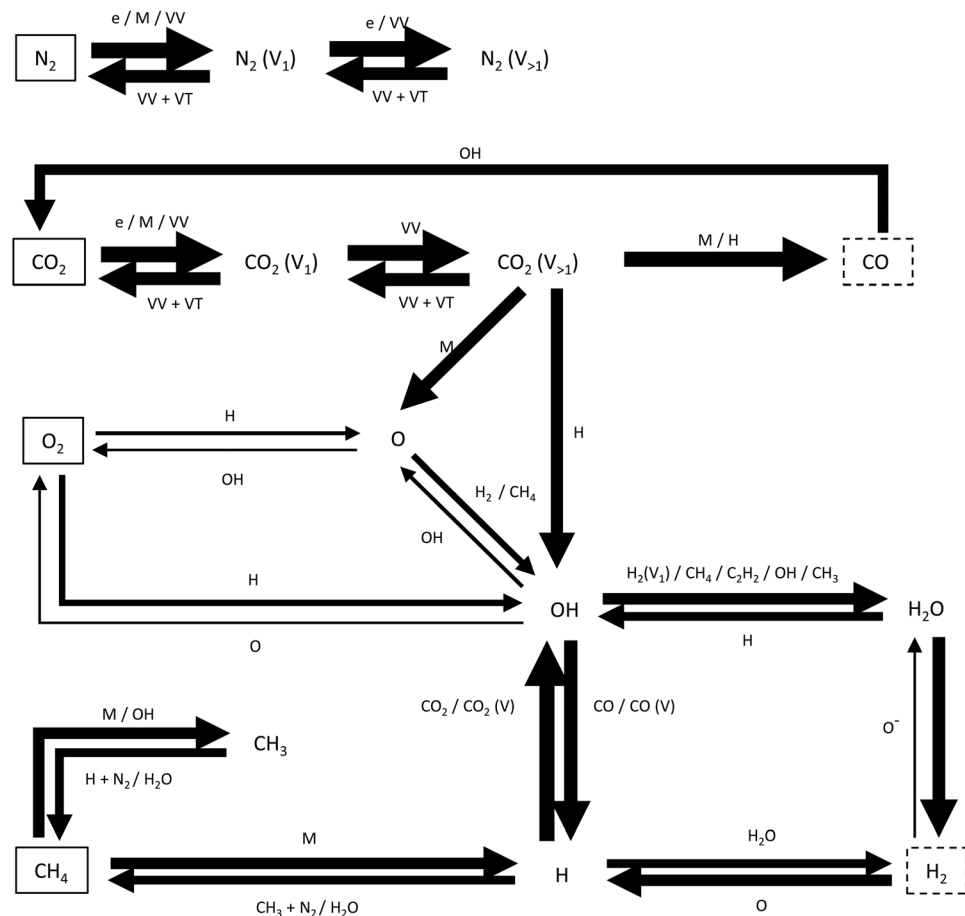
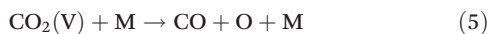


Fig. 8 Main reaction pathways for the conversion of CO_2 , CH_4 and O_2 into CO and H_2 , through various intermediate species, as determined from the simulations with 73% N_2 , 10% CO_2 , 10% CH_4 and 7% O_2 inside the arc. The thickness of the arrow lines indicates the importance of the reactions. See details in ESI (Fig. S20–S27†).

the energy efficiency of the conversion process. It is therefore important to have a strong non-equilibrium between the vibrational and translational (gas) temperature in the plasma.

After CO_2 has reached high enough vibrational energy, it dissociates through reaction with either H [eqn (4)] or a neutral plasma species [eqn (5)].



The lower vibrational levels ($\text{V}_{<14}$) react mostly through eqn (4), while the higher vibrational levels ($\text{V}_{\geq 14}$) react almost exclusively through eqn (5), in which M is mostly N_2 , because of its highest fraction in the mixture.

In parallel, O and OH are also produced in the plasma, from the added O_2 in the mixture, through the reaction in eqn (6), which is the most important O_2 loss process.



The produced O atoms react with H_2 [eqn (7)] and CH_4 [eqn (8)] into OH .



The formed OH can react with several species, such as $\text{H}_2(\text{V}_1)$ [eqn (9)], CH_4 [eqn (10)], C_2H_2 [eqn (11)], OH [eqn (12)] and CH_3 [eqn (13)] to form H_2O .



The H atoms, produced in eqn (7) and (9), react with H_2O to H_2 , following eqn (14).



Importantly, the OH radicals do not only contribute to the H_2O and H_2 production, but also to the loss of CO , which will

partially react back to CO₂ (see eqn (15), and thick arrow line in the upper part of the diagram).



The above reactions summarize how CO₂ is converted and how CO and H₂ are formed, as well as how O₂ and N₂ are involved in these pathways. In addition, CH₄ is converted in some reactions involving OH, but these are only partially responsible for the CH₄ conversion. Indeed, CH₄ is mainly split into H and CH₃ by thermal reactions with various molecules (M), mostly N₂, H₂ and H₂O. *Vice versa*, CH₃ and H can also recombine back into CH₄ in three-body collisions with multiple species as third body, *e.g.*, N₂ and H₂O, as indicated in Fig. S23 of the ESI.†

In addition, the H atoms formed from CH₄ splitting also react with O₂ and CO₂(V) into O and OH, which cascade towards H₂O and H₂ as described above. Next to the H atoms, the CH₃ radicals are a major product formed from CH₄ splitting, and they can react further into a range of different species, such as C₂H₂, C₂H₄, CH₂O, CH₃OH, ... However, because the latter are only formed in low quantities (*cf.* Fig. 3 and 4), they are not displayed in the pathways of Fig. 8.

It should be noted that the pathways drawn in Fig. 8 apply to the specific gas mixture of 73% N₂, 10% CO₂, 10% CH₄ and 7% O₂. Changing the O₂ fraction affects the chemistry, as discussed above, and this will be reflected in the pathways. However, for all O₂ fractions investigated, the changes are only in relative size of the arrows, while the pathways themselves are the same. On the other hand, without O₂ some differences are observed in the pathways. The H atoms obtained from CH₄ splitting will not react (so much) with O₂ as there is less O₂ present (only some fraction produced from CO₂ splitting). Therefore, the reverse reaction is much more important in this case, leading to a lower CH₄ conversion, as indeed observed in the experiments (*cf.* Fig. 2). In addition, the reaction between H and O₂ will be less important, because the O₂ present only originates from CO₂ splitting, so there is less OH being produced, which also leads to a lower reverse reaction from CO to CO₂. There is still some production of OH and H₂O, as CO₂ is still converted in O atoms that can form OH and H₂O, but only in much lower quantities. This also explains why the conversion of CH₄ increases and the conversion of CO₂ decreases at 11% O₂ fraction. The amount of O₂ in the mixture is then higher than that of CH₄, and it will quickly consume the produced H atoms from CH₄ splitting, resulting in high OH amounts, which convert CO back into CO₂, effectively decreasing its conversion. A similar behaviour was reported upon H₂O addition to a DBD plasma operating in CO₂.²⁵

Conclusions

In this paper, we investigated the conversion of CH₄ and CO₂ into CO and H₂ in a GAP, upon addition of O₂ and N₂ to the mixture, showing promising results for DRM. O₂ addition results in a higher CH₄ conversion, while the CO₂ conversion

was only slightly reduced upon adding high O₂ fractions. The CO and H₂ yields were also determined: the CO yield rises upon addition of O₂, while the H₂ yield slightly decreases. The energy cost also drops with increasing O₂ fraction, which is interesting for future applications from an economical point of view. Using an O₂ fraction larger than the CH₄ fraction, however, results in a lower CO₂ conversion, because CH₄ is fully oxidized into CO₂, thus reducing the net CO₂ conversion. This also increases the energy cost. The best results were obtained for a high O₂ and CH₄ fraction, *i.e.*, a mixture of 61.5% N₂, 15% CH₄, 10% CO₂ and 13.5% O₂. At these conditions, the CO₂ and CH₄ conversion reached 44 and 96%, respectively, yielding an energy cost of 13.4 kJ L⁻¹ or 3.4 eV per molecule. The benefit of adding O₂ to the mixture, *i.e.*, to increase the CH₄ conversion and to reduce the energy cost, is slightly outweighed by the drop in H₂/CO ratio of the produced syngas. The results can possibly be further enhanced by a change in the reactor design, to allow more gas passing through the arc plasma. This is especially important for improving the CO₂ conversion, because the CH₄ conversion largely proceeds by thermal reactions, so it also occurs in the hot region around the arc plasma.

Next to experiments, we also performed simulations for the different conditions studied experimentally. These simulations allow to obtain insight in the plasma chemistry, and to reveal the underlying reaction pathways. The overall conversion was obtained as the combination of conversion in the plasma arc and thermal conversion in the area around the arc. Inside the arc, both CO₂ and CH₄ can reach high conversions, but as the fraction of gas passing through the arc is limited, the thermal conversion outside the arc proved to be very important in the overall CO₂ and CH₄ conversion. The reaction pathways elucidated in this study confirm the ladder climbing process for the conversion of CO₂ and how this ties into the rest of the plasma chemistry. The H and OH radicals were found to be important in the mechanism to convert CO back into CO₂, and this lowers the CO₂ conversion, which is influenced by the O₂ fraction present in the gas mixture.

In general, our work illustrates that the addition of O₂ to the DRM gas mixture greatly improves the results. When benchmarking our results with the available literature, we obtain the highest CH₄ conversion, and a very competitive energy cost, when compared to other types of plasma reactors.

Adding N₂ was needed to create a stable plasma, and it also mimics emissions from industrial plants. In addition, N₂ is found to assist in the CO₂ conversion, but part of the applied electric power is also wasted into excitation and ionization of N₂ and can therefore not all be used for CO₂ and CH₄ conversion. This indicates that if the fraction of N₂ in our mixture could be reduced, we expect to reach lower energy costs. This will be investigated in future work.

Conflicts of interest

There are no conflicts to declare.

Acknowledgements

We acknowledge financial support from the European Research Council (ERC) under the European Union's Horizon 2020 research and innovation programme (grant agreement No 810182 – SCOPE ERC Synergy project), the Excellence of Science FWO-FNRS project (FWO grant ID GoF9618n, EOS ID 30505023), and the FWO postdoctoral fellowship of M. A. (Grant number 12M7118N). This work was carried out in part using the Turing HPC infrastructure at the CalcUA core facility of the Universiteit Antwerpen, a division of the Flemish Supercomputer Center VSC, funded by the Hercules Foundation, the Flemish Government (department EWI) and the University of Antwerp.

Notes and references

- 1 R. Snoeckx and A. Bogaerts, *Chem. Soc. Rev.*, 2017, **46**, 5805–5863.
- 2 M. Scapinello, E. Delikonstantis and G. D. Stefanidis, *Chem. Eng. Process: Process Intensif.*, 2017, **117**, 120–140.
- 3 F. A. Rahman, M. M. A. Aziz, R. Saidur, W. A. W. A. Bakar, M. Hainin, R. Putrajaya and N. A. Hassan, *Renewable Sustainable Energy Rev.*, 2017, **71**, 112–126.
- 4 G. Centi and S. Perathoner, *Catal. Today*, 2009, **148**, 191–205.
- 5 B. Hu, C. Guild and S. L. Suib, *J. CO₂ Util.*, 2013, **1**, 18–27.
- 6 S. Heijckers, R. Snoeckx, T. Kozák, T. Silva, T. Godfroid, N. Britun, R. Snyders and A. Bogaerts, *J. Phys. Chem. C*, 2015, **119**, 12815–12828.
- 7 R. Snoeckx, S. Heijckers, K. Van Wesenbeeck, S. Lenaerts and A. Bogaerts, *Energy Environ. Sci.*, 2016, **9**, 999–1011.
- 8 M. Ramakers, S. Heijckers, T. Tytgat, S. Lenaerts and A. Bogaerts, *J. CO₂ Util.*, 2019, **33**, 121–130.
- 9 J.-L. Liu, H.-W. Park, W.-J. Chung, W.-S. Ahn and D.-W. Park, *Chem. Eng. J.*, 2016, **285**, 243–251.
- 10 P. Thanompongchart, P. Khongkrapan and N. Tippayawong, *Period. Polytech., Chem. Eng.*, 2014, **58**, 31.
- 11 N. Rueangjitt, T. Sreethawong and S. Chavadej, *Plasma Chem. Plasma Process.*, 2008, **28**, 49–67.
- 12 B. Zhu, X.-S. Li, J.-L. Liu and A.-M. Zhu, *Int. J. Hydrogen Energy*, 2012, **37**, 16916–16924.
- 13 X. Zhu, K. Li, J.-L. Liu, X.-S. Li and A.-M. Zhu, *Int. J. Hydrogen Energy*, 2014, **39**, 13902–13908.
- 14 T. Nunnally, K. Gutsol, A. Rabinovich, A. Fridman, A. Gutsol and A. Kemoun, *J. Phys. D: Appl. Phys.*, 2011, **44**, 274009.
- 15 E. Cleiren, S. Heijckers, M. Ramakers and A. Bogaerts, *ChemSusChem*, 2017, **10**, 4025–4036.
- 16 M. Ramakers, G. Trenchev, S. Heijckers, W. Wang and A. Bogaerts, *ChemSusChem*, 2017, **10**, 2642–2652.
- 17 S. Pancheshnyi, B. Eismann, G. J. M. Hagelaar and L. C. Pitchford, *Computer code ZDPlasKin*, University of Toulouse, LAPLACE, CNRS-UPS-INP, Toulouse, France, 2008. <http://www.zdplaskin.laplace.univ-tlse.fr>.
- 18 I. T. Trotsuş, T. Zimmermann and F. Schüth, *Chem. Rev.*, 2014, **114**, 1761–1782.
- 19 P. L. Spath and D. C. Dayton, *Preliminary Screening – Technical and Economic Assessment of Synthesis Gas to Fuels and Chemicals with Emphasis on the Potential for Biomass-Derived Syngas*, Golden, CO (United States), 2003.
- 20 G. Trenchev, S. Kolev, W. Wang, M. Ramakers and A. Bogaerts, *J. Phys. Chem. C*, 2017, **121**, 24470–24479.
- 21 Q. Wang, B.-H. Yan, Y. Jin and Y. Cheng, *Plasma Chem. Plasma Process.*, 2009, **29**, 217–228.
- 22 J. Q. Zhang, J. S. Zhang, Y. J. Yang and Q. Liu, *Energy Fuels*, 2003, **17**, 54–59.
- 23 M. E. Gálvez, A. Albarazi and P. Da Costa, *Appl. Catal., A*, 2015, **504**, 143–150.
- 24 T. Kozák and A. Bogaerts, *Plasma Sources Sci. Technol.*, 2014, **23**, 045004.
- 25 R. Snoeckx, A. Ozkan, F. Reniers and A. Bogaerts, *ChemSusChem*, 2017, **10**, 409–424.